throughout the United States (n = 79). The test panel of 40 HIV-1–positive sera included specimens from 12 asymptomatic seropositive patients (CDC group II), 13 patients with generalized lymphadenopathy (CDC group III) or AIDS-related complex (ARC; CDC group IV-A), and 15 patients with overt AIDS [CDC group IV-C or IV-D; (27)]. The sera from Zairian HIV-1–infected patients and healthy Zairian controls were collected in Kinshasa in 1983 and have been all characterized (26). The HIV-2–positive sera were collected in Guinea Bissau in 1980 and characterized by immunoblotting and immunofluorescence against HIV-1, HIV-2, and SIV antigens (28). The panel of 48 control sera from Americans included 24 healthy laboratory personnel and 24 healthy homosexual men. Specimens were coded, divided into aliquots, and stored at −20°C until tested. Using HIV-1 gp41 (peptide 1 in Table 1) investigators at WHO found the ELISA to be as sensitive as three commercial kits when they tested 22 HIV-1–positive sera from patients in Zambia. No false positives were observed in tests of 411 sera from normal patients, including 32 pregnant women, from Nigeria.
18. J. B. McCormick *et al.*, *Am. J. Trop. Med. Hyg.* **36**, 102 (1987).
19. M. Alizon, S. Wain-Hobson, L. Montagnier, P. Sonigo, *Cell* **46**, 36 (1986).
20. M. Guyader *et al.*, *Nature (London)* **326**, 662 (1987).
21. S. Wain-Hobson *et al.*, *Cell* **40**, 9 (1985).
22. The single serum sample from an American that was reactive with HIV-2 peptide 5 was collected in San Diego in 1985 from a 35-year-old white male homosexual ARC patient. He had no history of travel to Africa or contact with Africans. Another sample collected in 1987 from the patient (now with overt AIDS) was still reactive with HIV-1 peptide 1 but nonreactive with HIV-2 peptide 5.
23. F. Clavel *et al.*, *Nature (London)* **324**, 691 (1986).
24. V. Hirsch, N. Riedel, J. I. Mullins, *Cell* **49**, 307 (1987).
25. J. M. Coffin, *ibid.* **46**, 1 (1986); S. Benn *et al.*, *Science* **230**, 949 (1985); B. H. Hahn *et al.*, *Proc. Natl. Acad. Sci. U.S.A.* **82**, 4813 (1985).
26. F. Brun-Vézinet *et al.*, *Science* **226**, 453 (1984).
27. Centers for Disease Control, *Morbid. Mortal. Weekly Rep.* **35**, 334 (1986).
28. P. N. Fultz *et al.*, Third International Conference on AIDS, Washington, DC, 1987, abstr. MP.72.
29. L. Ratner *et al.*, *Nature (London)* **313**, 277 (1985); B. R. Starcich *et al.*, *Cell* **45**, 637 (1986); R. Sanchez-Pescador *et al.*, *Science* **227**, 484 (1985).
30. Supported in part by USPHS grants AI-07007 and NS-12428 and NIH training grant T32-NS-07078 (J.W.G.). We thank P. Marx and M. K. Axthelm for providing monkey sera and A. B. Truax for providing human sera.

7 July 1987; accepted 1 August 1987

The Surface Composition of Charon: Tentative Identification of Water Ice

Robert L. Marcialis, George H. Rieke,* Larry A. Lebofsky

The 3 March 1987 Charon occultation by Pluto was observed in the infrared at 1.5, 1.7, 2.0, and 2.35 micrometers. Subtraction of fluxes measured between second and third contacts from measurements made before and after the event has yielded individual spectral signatures for each body at these wavelengths. Charon's surface appears depleted in methane relative to Pluto. Constancy of flux at 2.0 micrometers throughout the event shows that Charon is effectively black at this wavelength, which is centered on a very strong water absorption band. Thus, the measurements suggest the existence of water ice on Pluto's moon.

The current season of mutual events between Pluto and its satellite Charon presents the opportunity for many unique experiments. For example, monitoring of these events allows the determination of absolute sizes and bulk density of these bodies with unprecedented precision. It is also possible to separate the contributions of both bodies to the total observed light. A spectrum obtained during totality may be subtracted from the mean of spectra obtained just before and just after an event. The remainder is a spectrum of the Pluto-facing hemisphere of Charon alone. Both bodies rotate synchronously, which during a central event amounts to only about 2°. Any color variation therefore must arise from compositional differences between the two bodies, rather than a regional variation on the surface of an individual body.

Near-infrared spectrophotometry is a powerful diagnostic tool for the identification of ices on outer solar system bodies because of the strength of molecular transitions in the 1.0- to 2.5-μm region. On the basis of elemental abundances and the stability of ices, the candidate materials for solid surfaces are relatively few, and even filter photometry in the 1.0- to 2.5-μm region is highly diagnostic of surface composition. We report here observations of an occultation of Charon by Pluto with a near-infrared filter set selected to distinguish the most likely surface constituents.

The observations reported here were made with the Infrared Photometer and the Multiple Mirror Telescope Observatory (MMT) at Mount Hopkins, Arizona. This photometer uses an InSb detector cooled with liquid helium. Measurements were made through an aperture 8.7 arc sec in diameter, and relative to sky reference areas 10 arc sec above and below Pluto in elevation. The stars SAO 120107, HD 105601, and HD 129655 were used for absolute flux calibration.

Data on Pluto were recorded between 0730 and 1315 UT on 3 March 1987. The approximate geometry of the Pluto-Charon system for these times is indicated in Fig. 1. According to the ephemeris of Tholen *et al.* (1), this interval spanned the times from roughly 1 hour before first contact until fourth contact. Observations were terminated at approximately 1315 due to brightening of the sky. The sky was clear all night.

Because of the faintness of Pluto, it is currently impossible to obtain a continuous infrared spectrum of Pluto at reasonable signal-to-noise during the few short hours of a single eclipse event. We therefore observed with four filters, each of which has a spectral resolution of about 5%, or 0.1 μm (2). From previous work (3) methane was known to be the dominant absorber for the combined Pluto-Charon system. The two strongest bands for methane in the near-infrared are at 1.7 and 2.35 μm; two additional filters were used to measure the near-by continuum at 1.5 and 2.0 μm. The infrared photometer was set to cycle automatically through these filters; each cycle took approximately 15 minutes. After every two cycles a set of similar measurements was obtained on SAO 120599, a nearby G0V star expected to have colors identical to those of the sun. Our observations are summarized in Table 1 and depicted graphically in Fig. 2.

It should be noticed that the out-of-eclipse light curve slope persists during totality. This is in itself proof that the albedo "spots" first proposed by Marcialis (4, 5) do in fact reside on Pluto, and not on the satellite.

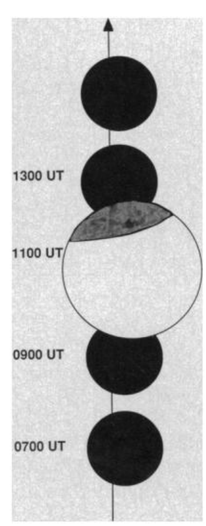

Fig. 1. Approximate geometry of the 3 March 1987 occultation of Charon by Pluto. The satellite was completely hidden for about 2 hours.

Lunar and Planetary Laboratory, University of Arizona, Tucson, AZ 85721.

*Also at the Steward Observatory, University of Arizona, Tucson, AZ 85721.

The occultation appears strongly in the two methane bands, indicating that a significant percentage of the light from the combined system comes from Charon. To our surprise, the event was virtually undetected at 2.0 μm. Evidently Charon is much darker than Pluto at this wavelength (which corresponds to methane continuum), so subtracting it from the system has negligible effect. If Charon contributed only a smooth continuum to the total light, then the strength of the methane band absorption would be expected to increase as the event reached totality; if Charon were as covered with methane as is Pluto, the band strengths would have remained the same throughout the event. Since neither situation held, Charon must be covered with some spectrally active material other than methane.

The spectral differences between Pluto and Charon are best illustrated by using the data in and out of occultation to derive plots of relative reflectance for the two objects, as shown in Fig. 3. The reflectances have been normalized to unity at 1.5 μm; errors in the 1.5-μm point have been absorbed in the error estimates at the other wavelengths.

Pluto shows the previously known strong methane absorptions at 1.7 and 2.35 μm, first identified by Cruikshank *et al.* (*6*) and confirmed by Lebofsky *et al.* (*7*). Since that time, the physical state of this methane has been under debate (*8, 9*). Buie (*10*) demonstrated that, at least in the 0.5- to 1.0-μm region, it is not possible to distinguish between the pure frost, pure gas, or the frost plus gas cases. However, the spectrum of Charon is radically different from that of Pluto.

Table 1. Measured flux densities (in millijanskys) versus time. The calibration of Campins *et al.* (*17*) has been assumed. Formal error bars were determined by computing the standard deviation of each datum from the out-of-eclipse light curve slope of 0.6% per hour. Thus, they reflect not only uncertainties due to photon statistics and the atmospheric extinction determination, but are a true estimate of the reproducibility of the data as well.

Time of observation (UT)	Wavelength (μm)			
	1.5	1.7	2.0	2.35
7.967	28.51 ± 0.31	15.55 ± 0.16	16.30 ± 0.57	4.47 ± 0.22
8.641	28.12 ± 0.31	15.92 ± 0.16	16.59 ± 0.57	4.69 ± 0.22
9.364	25.86 ± 0.33	14.74 ± 0.16	16.27 ± 0.57	4.60 ± 0.22
9.991	24.68 ± 0.27	13.21 ± 0.17	15.44 ± 0.57	3.43 ± 0.24
10.647	24.61 ± 0.27	13.09 ± 0.16	16.65 ± 0.41	3.63 ± 0.23
11.281	24.41 ± 0.33	13.04 ± 0.17	15.99 ± 0.57	3.57 ± 0.22
11.915	24.37 ± 0.33	12.89 ± 0.17	15.14 ± 0.59	3.53 ± 0.23
12.516	25.11 ± 0.27	13.89 ± 0.16	15.83 ± 0.59	4.17 ± 0.22
13.133	27.09 ± 0.27	15.41 ± 0.16	16.08 ± 0.60	4.69 ± 0.23

Several types of ices may be excluded by comparison of our data to laboratory spectra. These include not only CH_4 (see Pluto spectrum for its signature), but also CO_2 (2.0-μm absorption too shallow, no absorption at 2.35 μm); H_2S (2.35-μm absorption too shallow); NH_4HS (2.0- and 2.35-μm depths reversed); and NH_3 (1.5- and 1.7-μm depths reversed, 2.0- and 2.35-μm absorptions too deep).

The most plausible candidate is H_2O ice. Water ice has an extremely strong absorption at 2.0 μm, and another which is moderately strong at 2.4 μm (*11*). At 55 K, the 1.5-μm and 1.7-μm reflectances of water ice are similar (*12*), although at warmer temperatures the 1.65-μm absorption band is relatively weak. Figure 4 shows a spectrum of 55 K water ice with our data superposed. The agreement with the spectrum of Charon is good, although the relative flux at 1.5 μm still differs by about 2 standard deviations from that expected for pure, fine-grained ice.

The water absorption feature at 1.65 μm is known to deepen as grain size is increased (*12*). Further, our filter at 1.5 μm is located on the steep short-wavelength side of the 1.55-μm absorption. A small shift in the effective wavelength of the filter could result in a rather substantial change in the product of available flux and filter response. Although more detailed spectra may reveal other surface constituents, it is likely from our data that water ice dominates the infrared spectrum of Charon.

Presumably, both Pluto and Charon have been near one another since their formation. Why, then, should such a severe composition dichotomy exist?

Preliminary analysis of the partial events observed in 1985 and 1986 (*13*) shows the visual albedo of Charon to be about half that of Pluto. Thus Pluto is expected to have a lower surface temperture than Charon. If we assume a temperature of 50 K for Pluto,

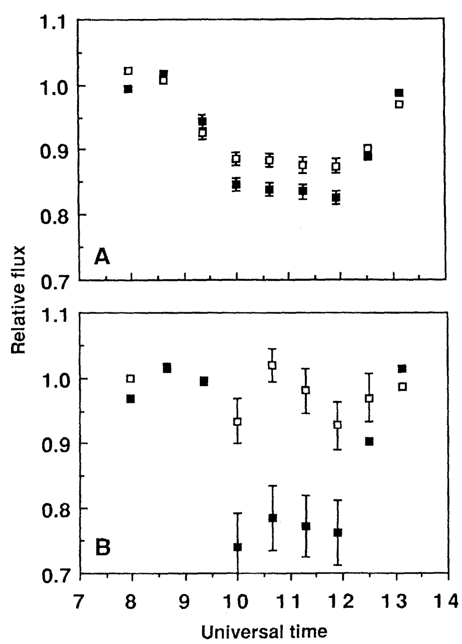

Fig. 2. Measured fluxes versus time, normalized to their mean values outside of the event; (**A**) 1.5-μm flux (□) and 1.7-μm flux (■); (**B**) 2.0-μm flux (□) and 2.35-μm flux (■). Note that at 2.0 μm the event is virtually undetected. At all wavelengths but 2.35 μm, an out-of-eclipse light curve slope of approximately 0.6% per hour is visible.

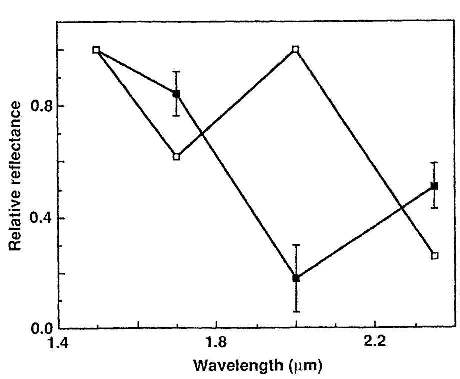

Fig. 3. Relative albedos for Pluto (□) and Charon (■), normalized to their individual reflectances at 1.5 μm. The small (~1%) error in the 1.5-μm measurement has been propagated to the other three wavelengths. Owing to its much stronger signal, formal errors in Pluto's spectrum are smaller than the plotted symbols.

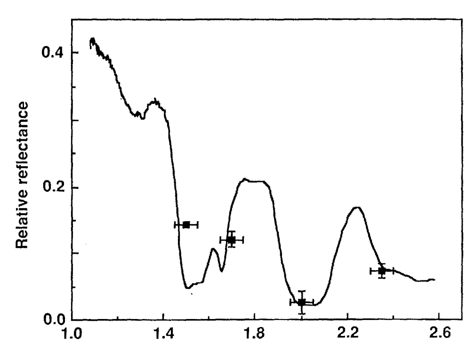

Fig. 4. Comparison of Charon reflectance to laboratory spectrum of water ice. The solid line is the spectrum of water frost at 55 K and the solid rectangles are the results of the present study. Horizontal bars indicate bandpass for each filter; vertical bars show estimates of overall errors in relative flux determination. Laboratory data from Fink and Larson (*12*).

Charon's temperature would be near 58 K. The vapor pressure of methane rises exponentially with temperature in this regime, from 3.5 μbar at 50 K to 59 μbar at 58 K (*14*). Since the root-mean-square thermal velocity of methane is about half of the escape velocity from Charon to infinity, and an even greater fraction of the velocity required for transfer through the inner Lagrange point onto Pluto, it is easy to show that Charon's inventory of methane would be lost on time scales short compared to the age of the solar system, whether by Jeans escape or hydrodynamic blowoff (*15*).

The details of the partitioning of methane between escape to infinity and transfer onto Pluto are as yet unclear, but escape of up to 22 km of methane from Charon can occur over the age of the solar system. After shedding several kilometers of methane, the surface of Charon would be expected to resemble a global "moraine," with the residuum composed of (cosmically abundant) water ice and a "slag" of darker carbonaceous or silicaceous impurities or both. This process could explain both the compositional difference and also why Charon's visual albedo is significantly less than that of Pluto (*16*).

REFERENCES AND NOTES

1. D. J. Tholen, M. W. Buie, C. E. Swift, *Astron. J.* **93**, 244 (1987).
2. "MMTO Visiting Astronomer Information," *Multiple Mirror Telescope Observatory Technical Report No. 13* (University of Arizona–Smithsonian Institution, Tucson, December, 1986), pp. 11–12.
3. B. T. Soifer, G. Neugebauer, K. Matthews, *Astrophys. J.* **85**, 166 (1980).
4. R. L. Marcialis, thesis, Vanderbilt University, Nashville (1983).
5. ——, *Bull. Amer. Astron. Soc.* **16**, 651 (1984).
6. D. P. Cruikshank *et al.*, *Science* **194**, 835 (1976).
7. L. A. Lebofsky, G. H. Rieke, M. J. Lebofsky, *Icarus* **37**, 835 (1979).
8. D. P. Cruikshank *et al.*, *Astrophys. J.* **217**, 1006 (1977).
9. U. Fink *et al.*, *Icarus* **44**, 62 (1980).
10. M. W. Buie and U. Fink, *ibid.* **70**, 483 (1987).
11. U. Fink and G. T. Sill, in *Comets*, L. Wilkening, Ed. (Univ. of Arizona Press, Tucson, 1982), pp. 164–202.
12. U. Fink and H. P. Larson, *Icarus* **24**, 411 (1975).
13. R. S. Dunbar and E. F. Tedesco, *Astron. J.* **92**, 1201 (1986).
14. G. N. Brown, Jr., and W. T. Ziegler, in *Advances in Cryogenics Engineering*, K. D. Timmerhaus and H. A. Snyder, Eds. (Plenum, New York, 1979), vol. 25, pp. 662–669.
15. See D. M. Hunten, *J. Atmos. Sci.* **30**, 1481 (1973); —— and A. J. Watson, *Icarus* **51**, 665 (1982).
16. D. J. Tholen, M. W. Buie, R. P. Binzel, M. L. Frueh, *Science* **237**, 512 (1987).
17. H. Campins, G. H. Rieke, M. J. Lebofsky, *Astron. J.* **90**, 896 (1985).

18. We thank the staff of the Multiple Mirror Telescope for their extra efforts in accommodating a one-night observing run and the 12 secondary mirror changes it entailed. This work was partially supported by NASA grants NGT-50048 and NSG-7114, and by the NSF. Observations reported in this report were obtained at the Multiple Mirror Telescope Observatory, a joint facility of the University of Arizona and the Smithsonian Institution.

12 May 1987; accepted 27 July 1987

Functional Regions of the Envelope Glycoprotein of Human Immunodeficiency Virus Type 1

MARK KOWALSKI, JOSEPH POTZ, LADAN BASIRIPOUR, TATYANA DORFMAN, WEI CHUN GOH, ERNEST TERWILLIGER, ANDREW DAYTON, CRAIG ROSEN, WILLIAM HASELTINE, JOSEPH SODROSKI

The envelope of the human immunodeficiency virus type 1 (HIV-1) plays a central role in the process of virus entry into the host cell and in the cytopathicity of the virus for lymphocytes bearing the CD4 molecule. Mutations that affect the ability of the envelope glycoprotein to form syncytia in CD4$^+$ cells can be divided into five groups: those that decrease the binding of the envelope protein to the CD4 molecule, those that prevent a post-binding fusion reaction, those that disrupt the anchorage of the envelope glycoprotein in the membrane, those that affect the association of the two subunits of the envelope glycoprotein, and those that affect post-translational proteolytic processing of the envelope precursor protein. These findings provide a functional model of the HIV envelope glycoprotein.

THE HUMAN IMMUNODEFICIENCY virus type 1 (HIV-1), also called HTLV-III or LAV-1, is the etiological agent of the acquired immune deficiency syndrome (AIDS) and related disorders (*1*). The viral envelope is synthesized as a 160-kilodalton (kD) (gp160) precursor glycoprotein, which is subsequently cleaved into 120-kD (gp120) and 41-kD (gp41) glycoproteins present on the virion particle (*2*). The gp120 exterior glycoprotein binds to the CD4 protein present on the surface of helper T lymphocytes, macrophages, and other cells (*3*), thus determining the tissue selectivity of viral infection. By analogy with other enveloped viruses, after the gp120 binds to CD4, virus entry is facilitated by an envelope-mediated fusion of the viral and target cell membranes.

The HIV-1 envelope glycoprotein is also responsible for at least some of the cytopathic effects of virus infection on CD4$^+$ cells in culture (*4, 5*). Expression of the envelope glycoprotein on the surface of infected cells mediates fusion events among CD4$^+$ cells via a reaction similar to that by which the virus enters the uninfected cell, leading to the formation of short-lived multinucleated giant cells. Syncytium formation is dependent on a direct interaction of the HIV-1 envelope with the CD4 protein (*3–5*).

To define the relation between the structure of the HIV-1 envelope glycoprotein and the ability to form syncytia, we introduced deletion and insertion mutations into a plasmid, pIIIenv3, that encodes the envelope glycoprotein derived from the HTLV-III_B strain of HIV-1. The gene was present on a plasmid that also encodes the *art* gene product (*4, 6*). CD4$^+$ and CD4$^-$ cell lines that expressed the HIV-1 *tat* gene product constitutively (*7*) were used as recipients in a transient transfection assay. To determine the size of the cell-associated and released proteins, we conducted radioimmunoprecipitation studies using antisera from AIDS patients or a goat antiserum to gp120 (*8*) and detergent-disrupted cells or cell-free supernatants prepared 48 to 72 hours after the cells had been transfected with pIIIenv3. The ability of the envelope proteins to bind to the CD4 protein and to induce syncytia was also examined.

The integral membrane protein (gp41) of HIV-1 differs from that of most retroviruses in the presence of additional sequences at the carboxyl terminus (*9*). The gp41 on the carboxyl-terminal side of the probable membrane-spanning region consists of a hydrophilic region (residues 724–745) and a terminal region (residues 745–856) of alternating hydrophilic and hydrophobic character (Fig. 1). Large deletions of either of these regions resulted in mutant *env* proteins that efficiently formed syncytia [see plasmids pIIIenvΔ(727–751), Δ813, and Δ753]. However, deletion of both of these regions (pIIIenvΔ727) resulted in very low levels of *env* protein production and loss of syncytium formation. When the deleted sequences were replaced by sequences derived from the *art* gene or by random sequences that have varying degrees of hydrophobic or hydrophilic character, syncytium induction was observed (for example, pIIIenvΔ722S, Δ725S, and Δ732S). The *art* protein-derived amino acid sequence could be introduced in the amino-terminal direction up to amino acid 705 without eliminating the ability of the mutated *env* protein to yield syncytia (pIIIenvΔ705S). However, substi-

M. Kowalski, J. Potz, L. Basiripour, T. Dorfman, W. C. Goh, E. Terwilliger, A. Dayton, C. Rosen, J. Sodroski, Laboratory of Biochemical Pharmacology, Dana-Farber Cancer Institute, and Department of Pathology, Harvard Medical School, Boston, MA 02115.
W. Haseltine, Laboratory of Biochemical Pharmacology, Dana-Farber Cancer Institute, and Department of Cancer Biology, Harvard School of Public Health, Boston, MA 02115.